Hindawi
Geofluids
Volume 2020, Article ID 9812597, 17 pages
https://doi.org/10.1155/2020/9812597

Research Article

The Hydrogeochemical Stratigraphy of Brines and Its Implications on Water Management in the Central Jordan-Dead Sea Rift Valley, Israel

Eliahu Rosenthal,[1] **Peter Möller**,[2] **Orna Buch-Leviatan**,[3] **and Moshe Politi**[3†]

[1]*The School of Geosciences, Tel Aviv University, Tel Aviv, Israel*
[2]*Helmholtz Centre, German Research Centre for Geosciences, GFZ, Section 3.4, Potsdam, Germany*
[3]*Zion Oil and Gas, Inc., Caesarea Industrial Park, Israel*
[†]*Deceased*

Correspondence should be addressed to Eliahu Rosenthal; elirose@netvision.net.il

Received 5 October 2019; Revised 31 October 2020; Accepted 25 November 2020; Published 17 December 2020

Academic Editor: Mercè Corbella

The exploratory borehole Megiddo-Jezre'el 1 (MJ1) was drilled in Israel, in the Bet She'an Valley which branches out from the Central Jordan Rift. It reached the depth of 5060 m and bottomed within the Upper Triassic Mohilla Fm. Following the increase of groundwater exploitation, the Cl^- concentrations increased and ionic ratios changed indicating inflow of Ca^{2+}-Cl^- brines, the origins of which were hitherto unknown. Data from the new MJ1 borehole revealed that rock porosities decrease with depth. Lowermost values of about 3% were interpreted from logs in Lower Jurassic and Triassic strata. The highest shut-in pressures were measured in the Upper Jurassic sequence raising the water much higher than the ground surface. Along the drilled section, there is a continuous downward increase in Cl^- concentrations in the range of 12-186 g Cl^-/l and a very clear stratification of brines. Data from the MJ1 borehole and from other exploration wells indicate that in the subsurface of the area, there are two definite source brines: Triassic brine and the Late Tertiary (so-called) Rift brine. Brines encountered in Jurassic and Cretaceous beds represent ancient mixtures of the two source brines involving various water-rock chemical transformations. Evidence of very high pressures in deep boreholes Devora 2A, Rosh Pinna 1, and MJ1 revealed the existence of a mechanism in which the deep brines are "piston-driven" upwards and possibly also laterally. The ongoing salinization of groundwater in the area is due to the inflow of the Late Tertiary Ca^{2+}-Cl^- Rift brines and not that of the Jurassic or Triassic brines. The hydrogeological and hydrochemical data from borehole MJ1 is of major importance for the management of groundwater resources in the Central Jordan Rift Valley and in the adjacent geologically connected areas.

1. Introduction

One of the major causes of the water crisis in Israel is the ongoing contamination of its groundwater resources by saline water bodies. The main deteriorating process occurring in groundwaters of the Jordan-Dead Sea Rift Valley and in adjacent connected areas is the upflow and migration of highly pressurized thermal Ca-chloride brines penetrating into fresh groundwater bodies [1]. In Israel, and particularly in the Rift and in branched-out areas, intensive exploitation of fresh groundwater has disturbed the natural equilibrium which prevailed between freshwater and saline water. The newly established groundwater flow regimes have facilitated the further migration of saline groundwater bodies, their participation in the active hydrological cycle, and the progressive contamination of fresh groundwater [2]. These processes were not anticipated by planners and water resources managers because there was no sufficient information about the

occurrence and the physical regimes controlling the migration of the brines.

A common feature of all groundwater bodies flowing in the Jordan-Dead Sea Rift Valley is that these are mixtures of low salinity or freshwater bodies with a Ca^{2+}-Cl^- saline brine, otherwise known as the "Rift brine." The origin of the low-salinity component may differ. South of the Dead Sea, it is usually the Lower Cretaceous paleowater from the so-called "Nubian sandstone aquifer" or recent floodwaters. Further northwards, the low-salinity component originates from the Cretaceous (Cenomanian-Turonian) and Tertiary (Eocene) groundwaters.

The saline Ca^{2+}-Cl^- component, i.e., the "Rift brine" [3], is identified by its high salinity and by typical ionic ratios such as $Q = Ca/(SO_4 + HCO_3 > 1$, $Na^+/Cl^- < 0.8$, $Mg^{2+}/Ca^{2+} < 0.5$, and $Cl^-/Br^- \ll 286$) [4]. Traditionally, Cl^-/Br is given as a weight ratio, whereas all the other ratios are calculated from meq/l values. The brine is characterized by high pressures and elevated temperatures and is encountered mainly (but not exclusively) along the western margins of the Rift, from the region of Lake Tiberias in the north to the northern Arava in the south. The chemical evolution was characterized by the increase of the Ca^{2+} concentrations as indicated by the raise of the Q value to values of $\gg 1$, decrease of the Na^+/Cl^- to values of <0.7, and Cl^-/Br^- decrease to values much lower than 286. All these chemical changes are clearly indicative of progressive inflow of pressurized and thermal Ca^{2+}-Cl^- brines which are encountered in the Jordan Rift Valley and in the adjacent areas which are in structural contact with the Rift [5].

Two types of brines were identified in the Rift [3]):

(i) Predominantly phreatic and nonthermal saline groundwater with $Mg^{2+}/Ca^{2+} > 1$ occurs along the eastern and southeastern shores of Lake Tiberias

(ii) Pressurized, thermal, and saline groundwater with equivalent ratios of $Mg^{2+}/Ca^{2+} < 1$ occurs mostly along the western margins of the Rift, between Lake Tiberias in the north and the Arava Valley in the far south. Freshwater-diluted Ca^{2+}-Cl^- brines mostly ascend near fault escarpments [1]

The study of groundwater salinization in the Rift started in the early 1960s [3]. Numerous researchers suggested a wide range of geological scenarios [6, 7].

Considering chemical and stable isotope data, it occurs that the water bodies contributing to saline groundwater in the Rift are as follows [6]:

(i) Recent Dead Sea water which is a primary evaporation brine with high $Mg^{2+} > Ca^{2+}$

(ii) Neogene seawater evaporation brine in the flooded Rift as represented by the Ha'On saline water characterized by $Mg^{2+} > Ca^{2+}$. This saline water flows out from springs and seepages along the eastern and southeastern shores of Lake Tiberias

(iii) Neogene-Tertiary brines with $Ca^{2+} > Mg^{2+}$ encountered in Tiberias Hot Springs and beyond the Bet She'an basin

(iv) Neogene to recent ablation brine with Na^+/Cl^- of about 1 encountered in the deep well Zemah 1 located at the southern tip of Lake Tiberias

(v) Deep-seated brines of the (Ca, Mg)Cl_2 type which are the subject of the present study

2. Objects of Investigations

As the result of the ongoing increase of groundwater exploitation in the Bet She'an and Harod Valleys since the early 1950s, the chemical composition of the exploited water changed due to variously diluted Ca^{2+}-Cl^- brines rising from depths and replacing the fresh groundwater. This process and its chemical details are similar for all water resources in the Rift, from Lake Kinneret in the north to the Arava in the south. In all these areas, scholars asked the same questions which remained equally unanswered because of a lack of information from horizons deeper than 800 m. These questions are as follows:

(i) Is there only one upflowing brine or are there several brines of similar composition but generated in different rock units and on different occasions?

(ii) What are the chemical compositions of the subsurface brine(s)?

(iii) In which rock units were these brines generated?

(iv) What is their updriving mechanism and at what rate?

(v) At what depth do the different brine bodies occur?

(vi) Assuming that answers are available to these questions, what would be the impact of upflowing brines on future regional plans for water exploitation?

The recent drilling of the deep exploratory borehole Megiddo-Jezre'el 1 (MJ1) supplied answers to many of the abovementioned questions. The present paper summarizes the results and their contribution to the understanding of the genesis and movement of brines in the Rift and in the structurally connected regions.

3. Materials and Methodology

The present study is based on the geological evidence from the recently drilled deep (5060 m) exploratory borehole Megiddo-Jezre'el 1 (MJ1), located 800 m south of Kibbutz Sde Eliahu, in the Bet She'an Valley, at Israeli coordinates 248240/703782, and Kelly Bushing (KB) at -180.1 m bsl. Until then, subsurface geological information in the area was limited only to the western and southern margins of the Bet She'an Valley, where it was derived from water wells such as Revaya 1-7, Bardala 1-2, and Mehola 5 (Cretaceous Judea Group aquifer) (Figure 1) [8]. The depths of these

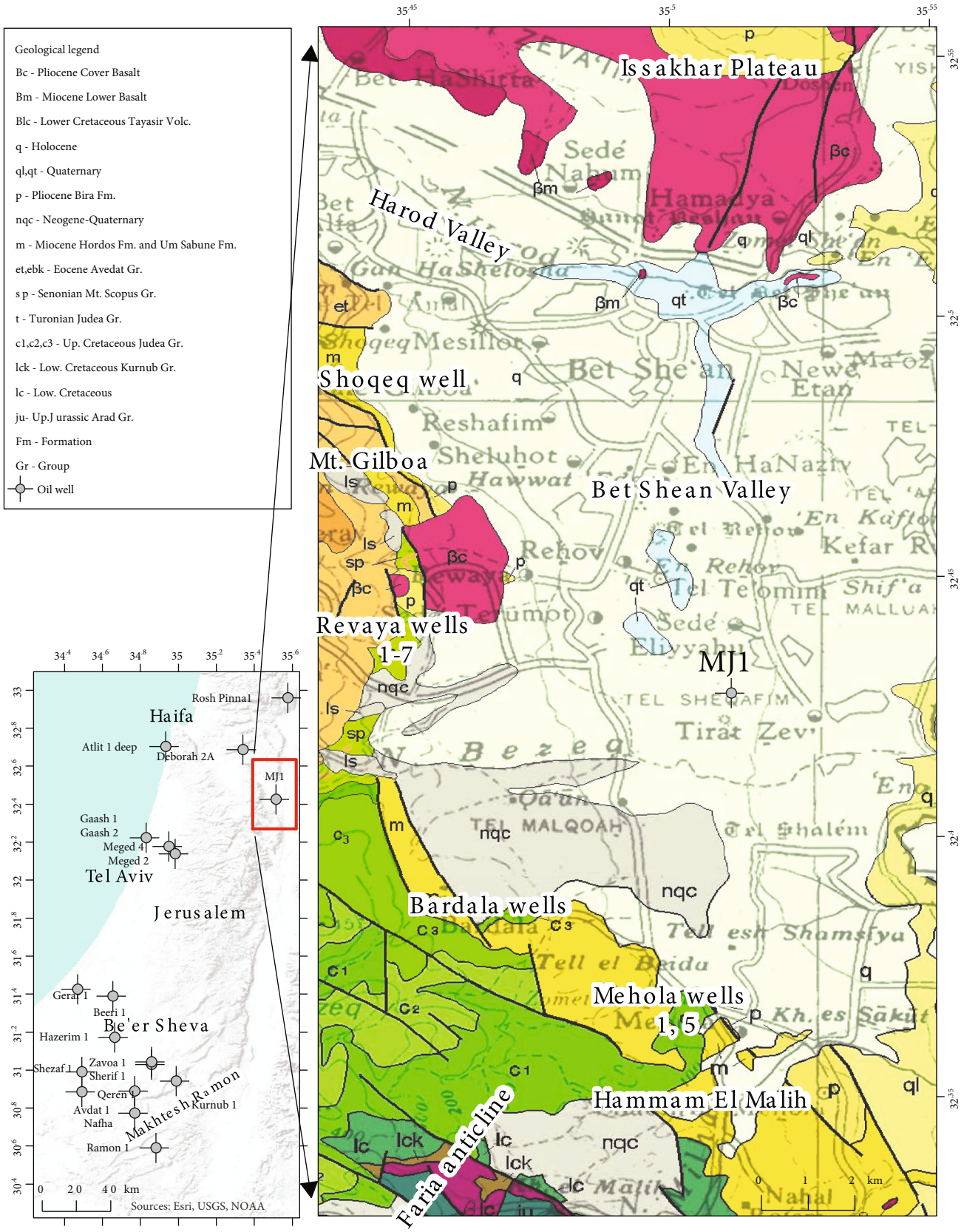

Figure 1: Geological location map. Geological data after [21].

water wells did not exceed 800 m. The northernmost well Shoqeq 1 exploits water from Tertiary Avedat Group limestones. There are no direct geological data from the central parts of the Valley. Gardosh and Brunner and Meiler et al. [5, 9] narrowed this information gap. They established the first subsurface structural model of the area based on the interpretation of seismic data. In borehole MJ1, the lithology and stratigraphy of the drilled section were established by careful examination of samples and on electrical logging. The major ions of all fluids encountered in the borehole during drilling operations were analyzed in the Geochemical Laboratory of the Geological Survey of Israel. The data are presented in Table 1. The accepted uncertainties of analyses were ±2% and, in few extreme and rare cases, up to ±3%. Information on porosities, temperatures, pressures, and Cl-concentrations were derived from logs [10], and Cl^- concentrations were deciphered from resistivity logs and calibrated with chemical analyses of water from bottom hole samples and from swabbing. Swabbing tests were run at preselected horizons (Figure 2). The chemical composition of fluids collected during the present drilling operations was compared with hydrochemical data from relevant water resources in the area, documented since the early 1960s (data from the files of the Hydrological Service of Israel, Mekorot, National Water Co., and from [10]). The triangular plot is built by Microsoft Excel with XLSTAT. The dendrogram shows the hierarchical ordering of data of the output from hierarchical clustering using the open domain R Code Team [11].

4. Geological and Hydrogeological Setting

The Bet She'an-Harod basin (BSB) (Figure 1) is a deep morphotectonic depression located at the eastern boundary of the Levant basin. It branches out of the Central Jordan Rift Valley, separating the calcareous Gilboa and Fari'a-Beqaot mountains to the west and south from the basaltic plateau of Issakhar to the north in the Eastern Lower Galilee. BSB is one in a series of intracontinental basins along the Dead Sea Rift (DSR) in the Middle East region whose tectonic development is associated with the development of the Dead Sea Transform (DST) fault system which is a plate boundary separating the African and Arabian plates [12]. Within the study area, two major structures influence the tectonic development of the region: the Syrian Arc System (SAS) to which the Fari'a-Beqaot structure belongs and the DST strike-slip fault along which the convergence of Africa and Eurasia takes place. The coexistence of SAS and DST shapes the eastern part of the Levant basin and its margins to the east [9, 11, 13–17]. The superposition of SAS and DST caused an abrupt change of the regional tectonic regime since the Miocene. The Fari'a-Beqaot anticline plunges towards NNE beneath the southern part of BSB. The most significant effects of active tectonics are the fast subsidence of the area surrounding DST, large thickness of accumulated fluvial and lacustrine sediments, and abundance of faults and fractures of different dimensions and ages [18].

According to Derin [19], the Triassic beds in Israel are only exposed in the southern part of the country in the erosion cirques of Makhtesh Ramon and Har Arif and were penetrated by 36 deep boreholes spread mainly over the southern and central parts of the country. Only 7 boreholes, including MJ1, were drilled in northern Israel. The Triassic Ramon Group [20] is characterized by large-scale marine oscillations which are the response to a regression of global extent. Due to alternations of the normal shelf and intertidal hypersaline to brackish environments in the Upper Triassic sequence, thick beds of gypsum/anhydrite occur in Israel in the Mohilla Fm and in Jordan in the Abu Ruweis Fm [20, 21]. Halite was found in borehole Ramallah. Triassic halite was also found in the southern Palmyrides in Syria and Lebanon [22]. The Triassic sequences display a north and eastward thickening, from 1100 m in the Negev to over 2600 m in borehole Devora 2A [23] and probably in MJ1 (base not reached). According to Greitzer [24], the salinities of brines in the Negev (Permian) and Ramon (Triassic) Groups increase northeastwards. This is consistent with Bentor [25] in which the ongoing emergence of the Arabo-Nubian massif throughout the Paleozoic-Lower Cretaceous time span created a hydrological gradient northward to structurally lower-lying areas.

The Triassic sequences display a trend of northward thickening, from about 1100 m in the south to more than 1700 m in boreholes Ramallah 1 and over 2600 m in Devora 2A (base not reached in these wells) [19]. Data from deep boreholes [19] indicate several hundred meters of thickening from the Coastal Plain eastwards. This thickened Triassic section was deposited in a basin defined as the "Judea-Galilee Low."

In large parts of the country, the Ramon Group contains five formations (from bottom-upwards): Yamin, Zafir, Ra'af, Saharonim, and Mohilla (of Scythian-Carnian age) built of marine carbonates, shales, and gypsum/anhydrite [19]. The depositional environment of the present study is the Mohilla Fm built of dolomite, anhydrite, and shales indicating a tidal environment ranging from a lagoon to a sabkha [19]. The thickness of the Mohilla Fm is remarkably variable. In the Negev and Dead Sea area, it is in the 20-200 m range, whereas in the north (in borehole Devora 2A), it reaches 870 m. Thick sequences of the Asher Volcanics occur in numerous boreholes between the Triassic and Jurassic sediments [19]. In borehole Atlit 1, this unit is 3.5 km thick, whereas in Devora 2A (closest to MJ1), it is 272 m. According to Derin [19] and personal comm. (2019), the Triassic sequence in central and northern Israel is identical to the Germano-Trias type spread throughout southern Europe, between Morocco in the west and Turkey in the east.

All Jurassic Fms are included in the Arad Group [26]. It stands out by the large variety of facies reflected in the occurrence of different lithologies. The environments of deposition range from shallow clastic shelf to deep open marine. The transition from the Triassic to the Jurassic is defined by a major angular unconformity causing erosional truncation and karstification of the underlying Triassic beds. These events created karst pockets filled with variegated clays—-Mishor Fm—penetrating deeply into the Upper Triassic beds. Further flushing and displacement of previously formed brines were either flushed west- and seawards or downwards to deeper stratigraphic levels in the subsurface. Hence, pre-Jurassic brines could have been preserved in few

Table 1: Chemical analyses of brines from previously drilled exploration wells and wildcats.

Location	Xing	Ying	Interval (m)	Stratigraphy	Ca^{2+}	Mg^{2+}	Na^{+}	K^{+}	Cl^{-} (mg/l)	SO_4^{2-}	HCO_3^{-}	Br^{-}	TDS
Nafha-2	127521	12211	2502-2539	Triassic	2906	1210	9196	400	22745	573	183		37213
Nafha-1	133144	14640	2347-2363	Triassic	2806	486	10916	227	23049	1154			38638
Devora 2A	182401	233122	4836-4864	Triassic	34890	1946	40169	402	129394	192	247	2099	209519
Gaash 2	133836	181436	5253-5273	Triassic	34469	5776	44742	3656	149003	240	122	2614	240622
Sherif 1	136565	49501	2849-2882	Triassic	16814	2128	34976	301	94146	577	122	782	149846
Shezaf 1	101140	33997	3503-3505	Triassic	10000	851	22084	277	55389	1009			89610
Gerar 1	117182	89413	3252-3265	Triassic	16794	1070	33987	66	86487	336	122	808	139670
Gerar 1	117.182	89.413	3240-3248	Triassic	21800	3190	41882	933	111000	350	242	804	179201
Qeren-1	101362	45036	2972-2992	Triassic	16580	2149	46179		105283	461	195		170847
Qeren-1	101.362	45.036	2919-2935	Triassic	15570	2094	42657	1079	99627	505	146	816	162494
Sherif 1	136.565	49.501	2234-2301	Triassic	1503	389	5860	156	11773	1538	122	92	21433
Meged 2	148271	171855	4365-4380	Triassic	1133	104	20500	1849	35450	671	102		59809
Meged 4	145978	186780	4318-4346	Triassic	34509	6104	45294	3789	146840	399	171	2802	239908
Rosh Pinna 1	204207	263055	2486-2586	Up. Trias.-Low. Jur.	4804	725	8000	375	22793	1162	370		38229
Rosh Pinna 1	204207	263055	3845-3864	Up. Trias.-Low. Jur.	27000	2920	33400	1160	105230	700	171		170581
Chemical analyses of liquids collected from borehole MJ1 during various phases of drilling operations													
ER58 ff: 25 hrs free flow	198240	203782	1228-1232.5	Low. Cretaceous	931	249	3734	160	7683	652	238		13347
ER29 ff: 1 day free flow	198240	203782	1775-1784	Up. Jurassic	674	50	33447	188	50890	75	1178	20	86522
ER31 ff: +7 days free flow	198240	203782	1775-1784	Up. Jurassic	686	20	17487	143	27930	160	998	20	47444
ER31 ff: +1/2 days free flow	198240	203782	1775-1784	Up. Jurassic	339	8	3363	104	5490	61	265	40	9670
ER34 ff: +2 hrs free flow	198240	203782	1775-1784	Up. Jurassic	470	64	2347	193	4355	414	100	45	7988
ER41 ff: +41.5 hrs free flow	198240	203782	1775-1784	Up. Jurassic	772	179	1700	120	3980	460	198	55	7464
ER51 ff: +82 hrs free flow	198240	203782	1775-1784	Up. Jurassic	766	185	1699	113	4017	471	197	60	7508
ER4 bb: ballast brine	198240	203782	3446-3468	Low. Jurassic	20	20	21262	30	32000	200		15	53547
ER8: mix of bb and ff	198240	203782	3446-3468	Low. Jurassic	12700	1500	20637	3043	62508	991		1110	102500
ER10: (ff) formation fluid	198240	203782	3446-3469	Low. Jurassic	24267	2906	34031	4871	103470	598		2015	172158
ER15 ff: 5 days free flow	198240	203782	3446-3470	Low. Jurassic	28734	2782	35747	4057	114930	585		2300	189135
ER16 ff: +2 days free flow	198240	203782	3446-3471	Low. Jurassic	31238	3108	37543	4209	123870	570		2410	202948
ER17 ff: +1 day free flow	198240	203782	3446-3472	Low. Jurassic	35041	3536	40254	4410	134463	497		2475	220676
ER18 ff: +1 day free flow	198240	203782	3325-3310	Low. Jurassic	30252	2802	36221	3946	123055	628		2240	199144
ER25 ff: +3 days free flow	198240	203782	3310-3325	Low. Jurassic	34052	3404	40273	4214	138715	384	27	3500	224569
DST bottom hole sample	198240	203782	4915.0	Up. Triassic	33254	4532	59700	523	171570	140	587	15	270321
ER2 BHS +24 hrs circulation	198240	203782	5000.0	Up. Triassic	11102	2398	54888	662	108814	240		645	178749

Table 1: Continued.

Location	Xing	Ying	Interval (m)	Stratigraphy	Ca^{2+}	Mg^{2+}	Na^{+}	K^{+}	Cl^{-} (mg/l)	SO_4^{2-}	HCO_3^{-}	Br^{-}	TDS
Chemical analyses from adjacent source													
Mehola 5 1969/70	19690	19745	94.0	Low. Cretaceous	40.6	35.0	50.0	6.0	74.1	27.0	278	0.54	511
Mehola 5 1969/70	19690	19745	100.0	Low. Cretaceous	48.1	79.4	177	14.8	354	116	231	0.23	1021
Mehola 5 1969/70	19690	19745	182.0	Low. Cretaceous	176	85	499	20.7	1227	109	280	0.12	2397
Mehola 5 1969/70	19690	19745	200.0	Low. Cretaceous	288	168	1036	41.1	2466	213	165	0.02	4376
Mehola 5 1970/71	19690	19745	265.0	Low. Cretaceous	480	92	1228	42.4	2698	219	220	0.04	4980
Mehola 5 1970/71	19690	19745	265, pumping	Low. Cretaceous	500	471	1058		3692	88	258	0.04	6067
Hammam el Malih spring 1969/70	19432	19414	Free flow	Up. Jur.-Low. Cret.	269	101	652	50.6	1525	311	189	0.06	3097
Ein el Jamal 1969/70	19732	19270	Free flow	Low. Cenomanian	162	89.8	590	34.3	1244	275	165	0.06	2560
Argaman well 20-18/12A 1969/70	20231	18023	Pumping	Up. Cenomanian	204	80.2	370	29	945	79.2	268	0.14	1976

ff = formation fluid; bb = ballast brine; DST = drill stem test; BHS = bottom hole sample; gwlevel = groundwater; bsl = below sea level; asl = above sea level.

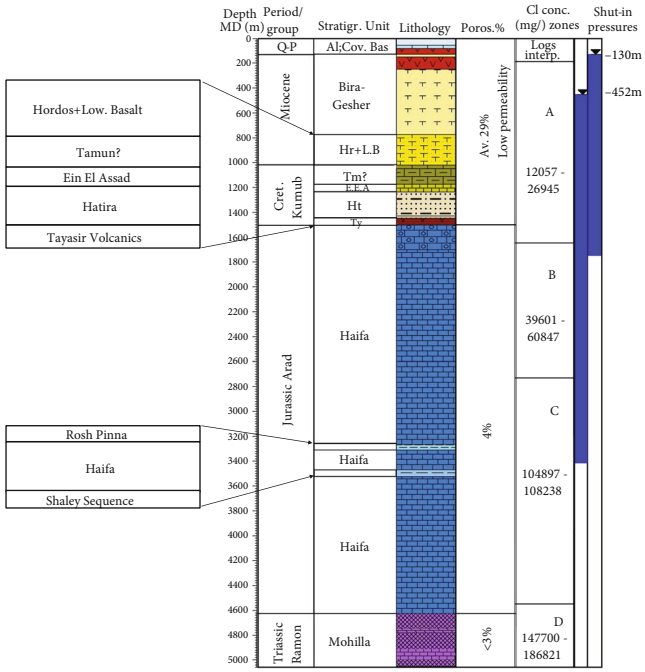

FIGURE 2: Lithology, porosity, shut-in pressure, and Cl^- concentrations.

natural reservoirs locally protected by geological conditions from flushing and from total evacuation [12, 27]. The maximal cumulative thickness of the Jurassic sequence including the offshore attains about 4700 m [26]. The Jurassic period stands also out by its basaltic and ultrabasic activity as evidenced in borehole Devora 2A (1025-1192 m) [19, 28].

At the beginning of the Lower Cretaceous (Kurnub Group), tectonic and erosive activities continue, and the whole area was uplifted [28–30]. A massive paleokarst surface developed along an unconformity in Upper Jurassic beds [31]. Considering lithostratigraphic evidence, it stands to reason that the Jurassic sequence was permeated through the karstic zone by large masses of water which flushed out the older bodies of brine. Intense faulting facilitated interaquifer connection and mixing of various water bodies. Interactions of seawater with basalts (Tayasir Volcanics) have generated Ca^{2+}-Cl^- brines.

During the Cenomanian, marine conditions prevailed over large parts of the Middle East and a thick sequence of carbonate sediments (Judea Group) was laid down. At the end of the Turonian, the folding of the Syrian Arch began causing the formation of basins and highs [32]. The fluids that permeated the Judea Group were probably seawater which might have locally undergone chemical changes due to water/rock interaction and gases from volcanic activity. These fluids were flushed out of the emerging land built of pre-Oligocene formations and, since the Quaternary, were replaced by natural recharge. At present, in the Judea Group, the groundwater is characterized by Cl^- concentrations which do not exceed 21 g/l. The values of Na^+/Cl^- and Cl^-/Br^- resemble those of seawater (0.86 and 286, respectively), and Q values are not higher than 3.

During the Mio-Pliocene, brines were mainly generated by repeated pre-Messinian ingressions of seawater. Following a deep penetration of the Tethys seawater, an inland lagoon was created in the nascent Rift. Evaporites precipitated in this lagoon, and their subsequent dissolution contributed to a new generation of brines. The Tertiary Hazeva and the Quaternary Dead Sea Groups are restricted to the Jordan-Dead Sea-Arava Rift Valley and are composed of up to 3000 m thick clastic, evaporite, and limnic sediments.

The regional exposed stratigraphic column of the Gilboa, Fari'a-Beqaot, and Issakhar mountains surrounding the Bet She'an basin includes the main rock units forming the regional aquifers that drain towards the Valley. These aquifers are 600-800 m thick Judea Group (Middle-Upper Cretaceous) built of karstic, highly permeable aquiferous limestones and dolomites. The approximately 400 m thick Eocene Avedat Group is characterized by chalks and limestones. The Neogene to Quaternary Tiberias and Dead Sea Groups comprising volcanic, lacustrine, marine, and continental rock units are also exposed in the area. Groundwater originating from Judea and Avedat aquifers exploited by boreholes is usually of the Ca^{2+}-HCO_3^- type and of low salinity (<400 mg Cl^-/l). Groundwater flowing in Neogene to Quaternary volcanic rocks and from interbedded lacustrine and continental strata are usually of higher salinity. Natural replenishment of the three regional aquifers occurs upon the exposed outcrops of the corresponding groups [33].

The natural outlets of all regional aquifers are two groups of springs. The Gilboa Springs emerge along the northeastern margins of Mt. Gilboa which is outlined by the Gilboa fault. The Mid-Valley Springs (MVS) emerge in the center of the BS Valley along a major morphotectonic lineament caused by subsurface faults branching out northwestwards from the Rift system [34]. The salinity of the MVS is at present <2000 mg Cl^-/l. When systematic quality monitoring began in the early 1950s, salinities were of the order of <500-800 mg Cl^-/l. It increased gradually in clear and proven dependence from regional freshwater exploitation by wells.

5. Results

5.1. The Exploratory Borehole MJ1. Based on geophysical evidence, borehole MJ1 was located on the northern plunge of the Fari'a-Beqaot anticline buried beneath the fill of the Bet She'an Valley (Figure 1). In the subsurface, the borehole is located near the intersection of longitudinal faults outlining the western rim of the Rift and faults branching archwise northwestwards out from the Rift system creating the Gilboa fault [9].

The total depth of the borehole is 5060 m, and the thicknesses of the penetrated rock sequences are as follows (Figure 2):

1020 m: Tertiary and Quaternary beds

483 m: Cretaceous Judea and Kurnub Group formations (incomplete due to structural reasons)

3123 m: Jurassic Arad Group formations

+430 m: Triassic Ramon Group formations

At the depth of 1020 m, there begins a major lacuna of the whole Avedat, Mt. Scopus, and the upper part of the Judea

Group. The calculated lacuna is about 1000-1250 m. There are two possible reasons for this lacuna—either a major fault or a major discordance extending over the Fari'a structure [27, 43]. There is quite strong evidence for the existence of a major fault which facilitates upflow of hot (72°C) and saline (4500 mg Cl^-/l) water at the depth of 1280 m. These unusual phenomena disappeared immediately after lowering the protective casing and isolating the inferred fault zone. A similar stratigraphic phenomenon was described from a nearby borehole Mehola 5.

Considering porosities interpreted from electrical logs run in the drilled section, the following depth intervals were outlined (Figure 2):

Quaternary-Miocene interval. In this interval, the porosities attain the highest values (aver. 32%). However, from acquired experience, it occurs that in the 0-865 m interval, permeabilities are very low and cannot be regarded as aquiferous.

Judea and Kurnub Groups. This depth range includes rock units related to the Judea Group (karstic carbonates) and to the Kurnub Group (sands and sandstones) (average porosity of 26%). These rock units could potentially be very good aquifers.

Arad Group, Haifa Fm. The thick calcareous Jurassic sequence is characterized by very low porosities (aver. 4%). The 3267-3310 m sequence of Rosh Pinna shales and the 3469-3523 m intervals stand out by its high content of shales. Fluids would only flow through faults and/or fissures.

Triassic Ramon Group. In the Mohilla formation (anhydrite/gypsum, dolomite, and limestone), porosities are even lower (aver. 3%) than in the overlying beds.

Two measurements of shut-in pressures are on record (Figure 2). At depth of 3414 m, the water level rose 2962 m to -452 m below KB (-632 m below MSL). Another measurement was made at depth of 1748 m, where the water level rose 1618 m to the level of 130 m below KB (-310 m MSL). This data is of the highest regional hydrological importance.

The recorded temperatures increase in borehole MJ1 (Figure 3).

From the surface down to a depth of about 100 m (down to the Cover Basalt), the temperature gradient is high (about 45°C/1000 m). Some temperature fluctuations were noticed which could be due to cooling effects by active groundwater flow from Mt. Gilboa and the Fari'a-Beqaot anticline in the west and southwest towards the center of the Bet She'an Valley. The presence of young volcanic bodies may explain the high temperatures at shallow depths. The Quaternary and Lower Cretaceous sections are characterized by low gradients of about ~10°C/1000 m. This depth zone contains mostly clastic rocks, and as observed in nearby well Mehola 5, fresh groundwater flow reduces the thermal gradient.

In the prevalent carbonate parts of the Jurassic and Triassic sequences, the temperature gradient is higher (27-28°C/1000 m). A certain increase in the gradient was noticed below the impermeable Rosh Pinna shales that presumably act as a sort of a hydrological barrier. In the Upper Jurassic down to the Rosh Pinna shales, the gradient rises to about 27°C/1000 m, whereas beneath the Rosh Pinna shales, the gradient changes to about 28°C/1000 m.

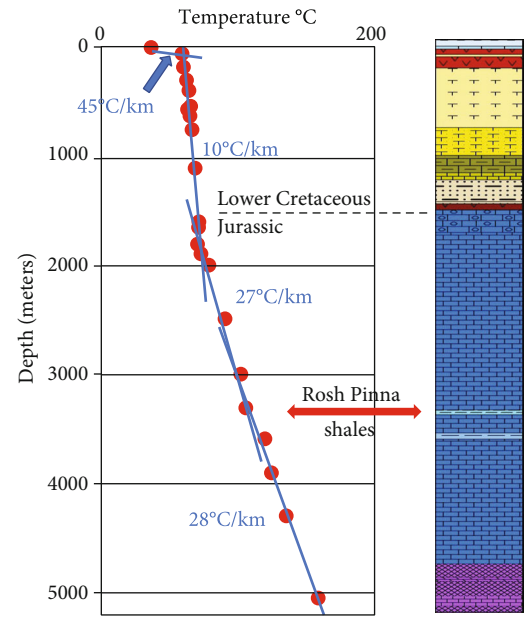

Figure 3: Temperature gradients in borehole MJ1. Color code like in Figure 2.

The water body in the upper parts of the Arad Group units cannot be regarded as brine because its Cl^- concentration is lower than that in seawater. Na^+/Cl^- and Q values differ from the values characterizing Ca^{2+}-Cl^- brines. Unlike the brine in Lower Jurassic and Triassic beds, this saline water body contains bicarbonate which indicates hydrological contact with active replenishment. $\delta^{18}O$ values were of -3.81 and -4.69. The data are presented in Table 1.

5.2. Changes in Porosity and Cl^- Concentrations. Measurements of water salinity along the drilled section of borehole MJ1 revealed a continuous increase in Cl^- concentrations with depth (Table 1). Four different zones of groundwater salinity could be outlined (from top-downwards, Figure 2):

Zone A. This fits almost perfectly with the sequence of post-Jurassic (Arad Group) strata which include Lower and Upper Cretaceous, Miocene, and Pliocene rock units. In this zone, porosities are particularly high in the aquiferous Kurnub Group.

Zones B and C. Within the very thick (3123 m) sequence of the Jurassic calcareous Haifa Fm, it is separated into two members by the Rosh Pinna shales (3270-3310 m): the Middle to Upper Jurassic member which is prevalently built of limestone with high porosity and low Cl^- concentration of its water and the lower member with enhanced contents of shale reflected by its lower porosity and higher salinity. The interbedded Rosh Pinna shales consist of gray to black fossiliferous detrital shales and marl interbedded with limestone and dolomite. The Upper Member overlying these shales has a much higher porosity, and the Cl^- concentration of its water is much lower. However, the very high pressures measured in the Jurassic beds underlying these shales could have caused the upward movement of these brines through the shales and into the overlying calcareous sequence.

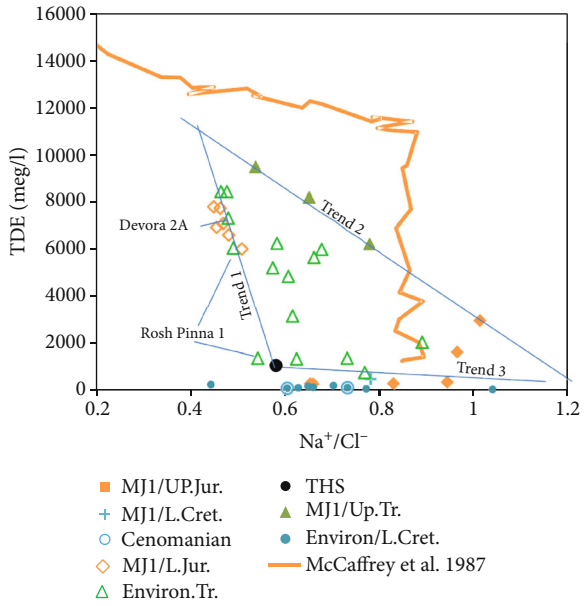

Figure 4: Total dissolved equivalents. TDE vs. Na^+/Cl^- showing dilution and mixing processes. Ratios are based on meq/l. Trend 1: mixing of Devora 2A and THS; trend 2: mixing of MJ1 and basaltic-rock water; trend 3: mixing of HTS and basaltic-rock water.

Zone D. This extends between 4550 m and +5060 m and contains brines with Cl^- concentration over 171 g/l. The top of this salinity zone is higher than the lithological boundary of the Triassic Mohilla Fm (at 4626 m) which is built mainly of massive dolomite and layers of anhydrite. Here again, the high pressure could have caused the upward movement of the brine into the overlying Lower Jurassic beds.

5.3. Comparison of MJ1 with Brines in the Vicinity. Following the definition of the hydrochemical identities of water bodies encountered in the study area by means of their characteristic ionic ratios, an attempt was made to verify—by means of cross plots between total dissolved equivalents (TDE) and various ionic ratios—whether these waters can be assembled into larger groups and the possible relations between them.

The TDE vs. Na^+/Cl^- plot (Figure 4; Table 2) reveals that trend 1 includes brines from the Lower Jurassic, i.e., ER4-25 and DST of borehole MJ1, Rosh Pinna 1, Devora 2A, and Tiberias Hot Springs (THS), members of the diluted Ha'On/-Tiberias brine family. The deepest Triassic samples (DST and ER2) follow trend 2.

The TDE vs. K^+/Cl^- plot suggests mixing of Upper Triassic and Lower Jurassic brines from borehole MJ1 but with a significant change in K^+/Cl^- (Figure 5(a)). The Devora 2A sample and the deep sample from borehole Rosh Pinna 1 plot near this trend. Different trends are shown by Upper Jurassic and Lower Cretaceous brines from MJ1. The red trend indicates the association of Rosh Pinna and THS brines.

The TDE vs. Na^+/K^+ plot reveals four trends of the Lower Jurassic, THS/shallow and Rosh Pinna (red lines), DST/Devora 2A, and Upper Jurassic brines (Figure 5(b)). Most Upper Jurassic and Lower Cretaceous brines cluster at both low TDE and Na^+/K^+ values.

Table 2: Chemical composition of Triassic brines in borehole MJ1. Cl^-/Br^- are in weight ratio; all other ratios are based on meq/l.

Parameter	Depth 4915 m	Depth 5000 m
Ca^{2+} (mg/l)	33254	21640
Mg^{2+} (mg/l)	4532	2094
Na^{2+} (mg/l)	59700	62248
K^+ (mg/l)	523	2748
Cl^- (mg/l)	171570	147900
SO_4^{2-} (mg/l)	140	200
HCO_3^- (mg/l)	587	490
SiO_2 (mg/l)	100	154
*r*Na/Cl	0.53	0.65
*r*Mg/Ca	0.22	0.15
rQ	132	88.5
*w*Cl/Br	11438	140.7

r = meq/l; *w* = mg/l.

The TDE vs. Mg^{2+}/Ca^{2+} plot shows a cluster of Lower Jurassic brines including deep Rosh Pinna (Figure 5(c)). All other groups of brines scatter widely. The red trend shows the combination of Rosh Pinna and THS.

The K^+/Cl^- vs. Na^+/Cl^- plot (in meq/l) reveals various trends in MJ1 (Figure 5(d)). The Upper Jurassic brines indicate mixing with basaltic water. The DST brines are lower in 1000 K^+/Cl^- than in seawater (18.6). The Lower Jurassic brine plots at low Na^+/Cl^-. The Triassic brines from the environment and the Lower Cretaceous brines scatter widely. HTS and the Rosh Pinna samples yield a mixing line.

6. Discussion

6.1. General Geochemical Considerations. All brines in the northern Rift basin and in the adjacent and structurally related areas represent evaporated seawater, the composition of which is altered by a number of chemical processes which are time-independent but depend on temperature and slightly on pressure. Mixing of brines and waters of different origins develop specific trends.

In the Na^+ vs. Cl^- plot, all data follow a common trend with a slope of about 1 suggesting that halite dissolution played an important role (Figure 6(a)). These basinal brines are of the Ca^{2+}-Cl^- type and are generated by reactions as follows:

$$\text{Plag} + 2Na^+ + 4SiO_2 \Leftrightarrow 2\text{Alb} + Ca^{2+} \quad (1)$$

$$2CaCO_3 + Mg^{2+} \Leftrightarrow CaMg(CO_3)_2 + Ca^{2+} \quad (2)$$

$$CaSO_4 \Leftrightarrow Ca^{2+} + SO_4^{2-} \quad (3)$$

$$CaCO_3 \Leftrightarrow Ca^{2+} + CO_3^{2-} \quad (4)$$

$$\text{K-feldspar} + Na^+ \Leftrightarrow \text{Alb} + K^+ \quad (5)$$

Due to these reactions, Na^+, K^+, Ca^{2+}, Mg^{2+}, SO_4^{2-}, and

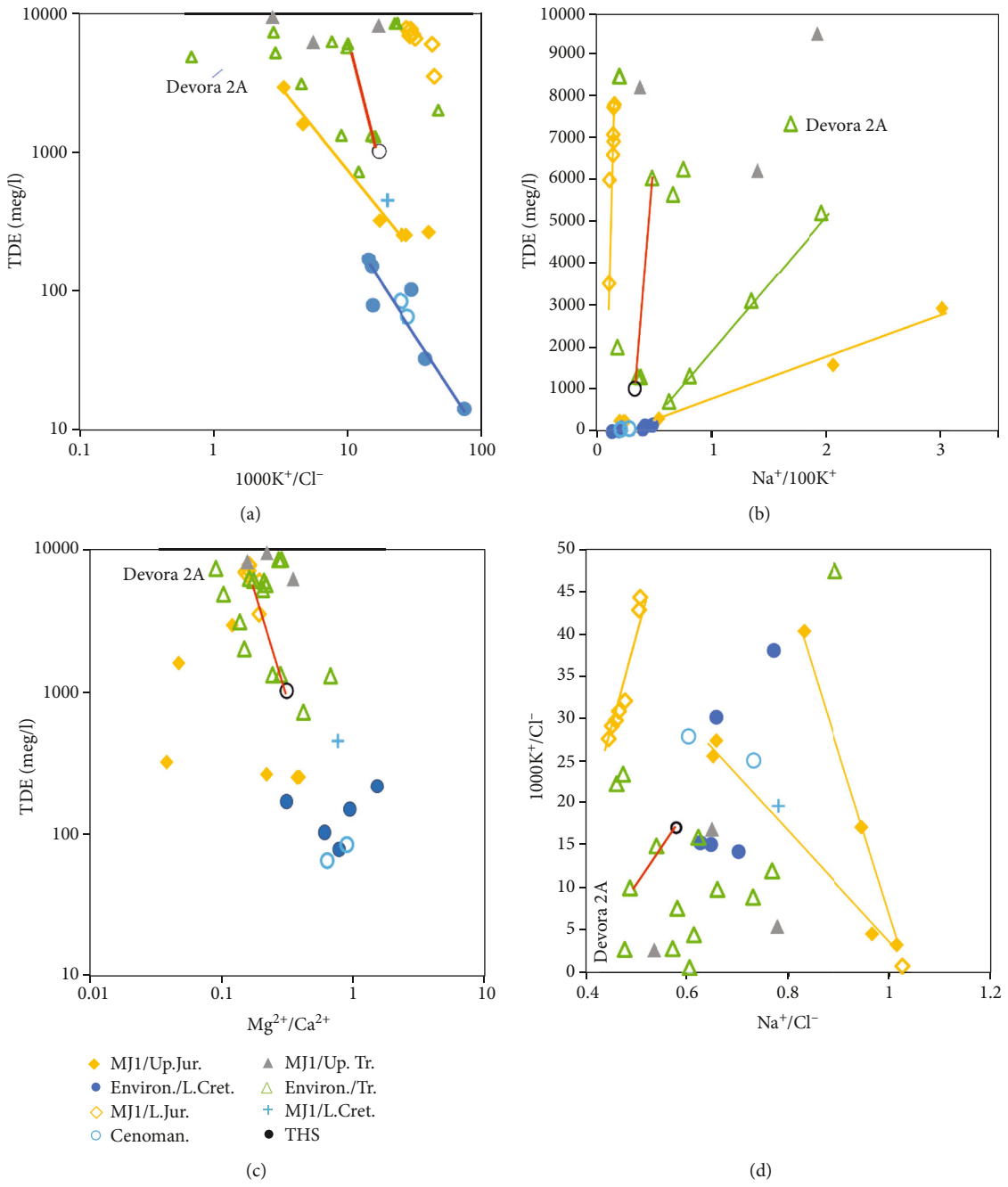

FIGURE 5: Various cross plots indicating correlations. Association of THS and shallow Rosh Pinna 1 is indicated by red lines. Devora 2A is not on this mixing line. The yellow, blue, and green lines indicate brines either mixing with other K^+-rich brines or interacting with K^+-rich evaporates. Ratios are based on meq/l.

HCO_3^- vary. Although diluted by freshwater, all brines in Table 2 are saturated with respect to carbonates (Figure 6(a)).

The slope of -1 in the exchange of Na^+ vs. Ca^{2+} in fluids proves albitization of plagioclase due to brine contact with basaltic matter (Figure 6(b)). The intercepts with the X-axis at 1 and 0.9 indicate halite fluids and seawater, respectively. In borehole MJ1, the Upper Jurassic brines, the brines from borehole Devora 2A, and some Lower Cretaceous Mehola 5 represent halite dissolution brines, whereas all the others are based on Na^+/Cl^- of about 0.9, i.e., originate from seawater or are mixtures of both sources.

6.2. Involvement in Dolomitization. Involvement in dolomitization is demonstrated in Figure 6(c). The value of Mg^{2+}/Ca^{2+} of 0.17 is in the range of dolomite formation. The drop in Mg^{2+} concentrations is mainly due to dilution with freshwater or basaltic water. The increase of Ca^{2+} by dolomitization facilitates elsewhere dedolomitization and precipitation of calcite and gypsum/anhydrite. Due to high Ca^{2+} in Triassic brines, their SO_4^{2-} and HCO_3^- are low (Table 1).

Reactions (1)–(4) do not occur in the same geological environment. Reaction (1) only occurs in the presence of basalts and tuffs, reaction (2) in limestones, and reactions

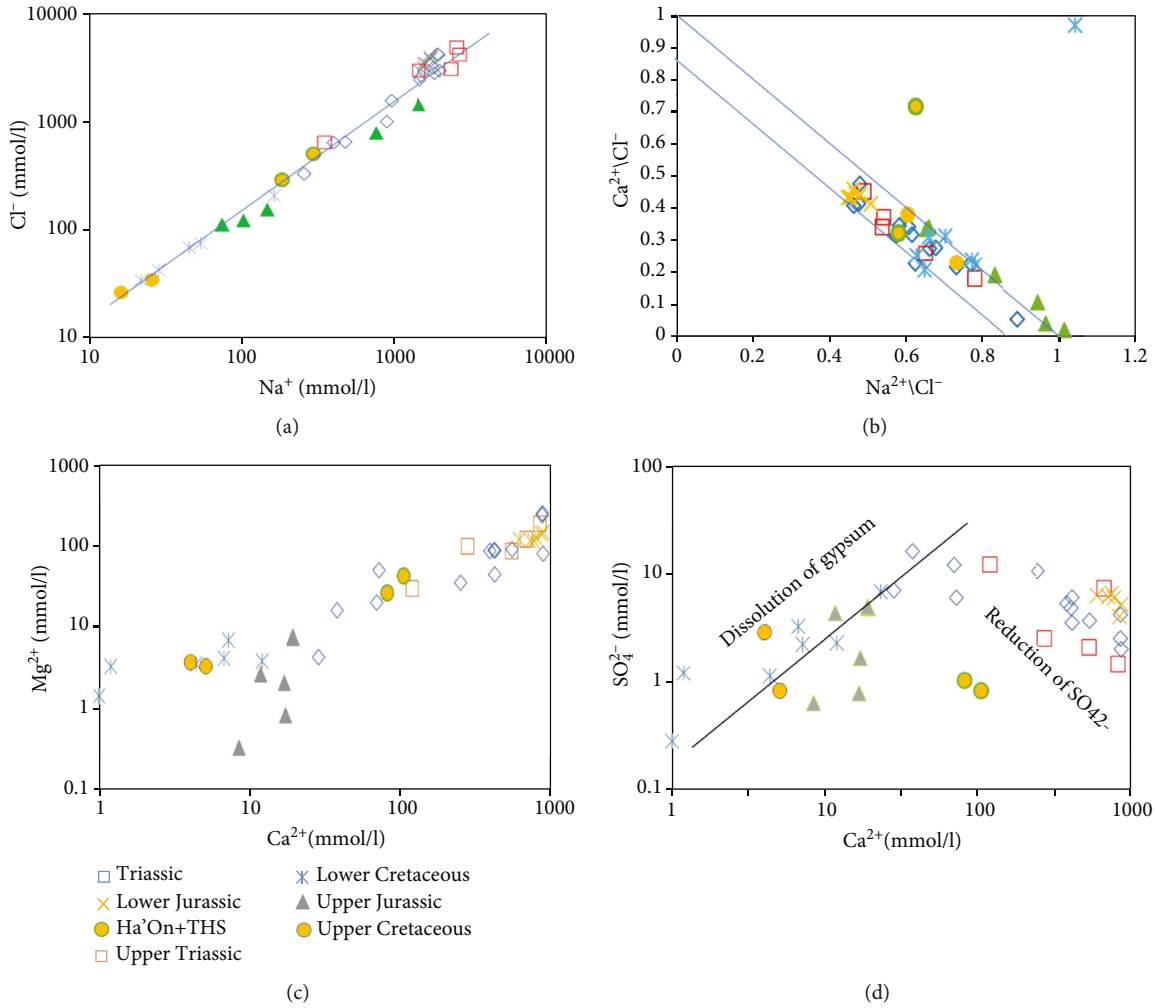

Figure 6: Cross plots of elements and element ratios indicating mineralogical processes. (a) Dissolution of halite or dilution of brine with freshwater. (b) The slope of the Mg^{2+} vs. Ca^{2+} plot with 0.17 is in the range of equilibria with dolomite. (c) Albitization of plagioclase. (d) Cross plots of Ca^{2+} vs. SO_4^{2-} reveal that three different trends: (i) dissolution of gypsum, (ii) sulfate dissolution, and (iii) bacterial sulfate reduction. Ratios are based on meq/l.

(3) and (4) in unsaturated solutions but in the presence of gypsum/anhydrite and calcite. Thus, the final equilibria of these reactions are randomly achieved in the rocks from which the samples for analysis are collected. Mixing with either higher or lower salinity water is common.

6.3. Sulfate. The proportional increase of sulfate and Ca in Figure 6(d) is best explained by the dissolution of gypsum/anhydrite.

6.4. Brines from Triassic Beds. Figure 6(a) portrays Cl^- concentrations in fluids of Upper Triassic formations collected from exploration boreholes. All fluids are of the Ca^{2+}-Cl^- type with high Q factors of up to 245 in borehole Gaash 2. In boreholes Devora 2A and Rosh Pinna 1, these brines are pressurized to 480 and 330 bar, respectively, and are thermal (162°C) [26]. The highest Cl^- concentration in MJ1 (171.6 g Cl^-/l) was encountered by bottom hole sampling at the depth of 4915 m (Table 2) in dolomite and anhydrite beds of the Triassic Mohilla Fm. This brine resembles those encountered in borehole Devora 2A and other boreholes penetrating the Mohilla Fm. The only difference is the very high Cl^-/Br^- values of 11438 in MJ1 indicating the presence of halite beds which should be regarded as a local occurrence in borehole MJ1 and was not found in Devora 2A. Such very high ratios were reported from Triassic sequences of gypsum interbedded with halite in Spain, Portugal, Switzerland, Germany, and Austria [35]. These brines were formed by massive ablation of halite and gypsum/anhydrite with significant influence of igneous processes [31]. The formation of such brines could have also been chemically linked to the very intensive Triassic volcanic activity in northern Israel, as evidenced from numerous boreholes (Asher, Yagur, Haifa, Atlit, and Devora 2A) (Fig. 2 in [29]). This is a typical Ca^{2+}-Cl^- brine with very high Q values of 132.4, $Na^+/Cl^- = 0.5$, and $Mg^{2+}/Ca^{2+} = 0.2$ (Table 2). The temperature of the brine was 160°C.

Bottom hole sampling at the depth of 5000 m revealed a brine that is of different composition. Its Cl^- concentration

is lower by 23 g/l, the concentration of K^+ is much higher (+2.23 g/l), the Cl^-/Br^- value decreases from 11438 to 140 indicating the absence of halite, and finally, it has a much lower Qfactor (88 instead of 132) (Table 2).

Triassic seawater is evaporated yielding increasing Cl^- and decreasing SO_4^{2-} concentrations. This latter trend is similar for the brines of boreholes Devora 2A, Rosh Pinna, and MJ1.

6.5. Brines from Jurassic Beds. Most saline Jurassic waters are compositionally comparable with seawater. The Jurassic seawater is diluted with freshwater causing decreasing SO_4^{2-} and Cl^- concentrations. The Jurassic Arad Group hosts at present two types of brines. In its lower part, the Cl^- concentration is in the range of 39-105 g/l with low concentrations of sulfate (380-1000 mg/l). These are typical Ca^{2+}-Cl^- brines with Q = 37-134, Na^+/Cl^- of 0.49-0.68, and low Cl^-/Br^- of 60-127. Such brines may have formed as the result of the evaporation of seawater. In the upper half of the Arad Group, the brines are of an entirely different type. These brines show Na^+/Cl^- values in the range of 0.78-1.18 and much higher Cl^-/Br^- values (111-248). Q values are much lower than in the deeper part of the group, i.e., in the 0.81-38 range. These brines could originate from seawater after dilution of evaporites. In borehole MJ1, no impervious layers separate between the Jurassic and Triassic sequences. In the Haifa Fm (1503-4626 m), two types of brines were encountered by swabbing in selected strata. The two brine bodies could be separated by the Rosh Pinna shales (Table 3).

During the tests, the shut-in pressure of the brine originating from Lower Jurassic beds rose to -632 m bsl and sometime later reached the level of -380 m bsl. Shut-in tests in Upper Jurassic beds indicated pressures of 12 atmospheres above KB, i.e., about -60 m bsl. This data is of primary importance for the management of the regional water resources of the area.

PHREEQC inverse modeling revealed that most brines in the Jurassic Fm seem to be derivatives of Triassic brines and basaltic water. Furthermore, it indicates that the brines encountered above the Rosh Pinna shales (sample ER51, 1775-1784 m, Table 1) could be related to the brines in Lower Jurassic beds (sample ER25 3310-3325 m) by dilution, dissolution, or precipitation of calcite (depending on the salinity of diluting solution), dissolution of anhydrite and silica, exsolution of CO_2, and cation exchange on clay particles of shales. The low-salinity end-member in modeling is represented by groundwater from well Beqaot 2.

6.6. Brines from Lower Cretaceous Beds. The chemical compositions of fluids derived from different Lower Cretaceous Fms (Kurnub/Hatira Group) elsewhere in the country are very similar. The Cl^- concentrations reach as high as 36 g/l. The values of Na^+/Cl^- and Cl^-/Br^- in these fluids (0.87-0.98 and 250-477, respectively) indicate that they could have evolved from seawater which did not reach the point of halite precipitation. The high Q = 13.3 could be the result of the involvement of both dolomitization and chemical reduction of sulfates.

Table 3: Averaged concentrations of chemical components and ionic ratios in the Jurassic (Arad Group) interval. Cl^-/Br^- are in weight ratio; all other ratios are based on meq/l.

Parameter	Above Rosh Pinna shales (6 samples) 1784-1775 m	Below Rosh Pinna shales (8 samples) 3468-3310 m
Ca^{2+} (mg/l)	617	24538
Mg^{2+} (mg/l)	84.3	2508
Na^+ (mg/l)	10007	33246
K^+ (mg/l)	143.5	3527
Cl^- (mg/l)	16110	104583
SO_4^{2-} (mg/l)	273	460
HCO_3^- (mg/l)	483	
SiO_2 (mg/l)	2.8	30
rNA/Cl	0.8	0.5
rMg/Ca	0.18	0.2
rQ	2.3	125
wCl/Br	74	50

r = meq/l; w = mg/l.

In the exposed and buried parts of the Fari'a-Beqaot anticline and close to borehole MJ1, groundwater originating from Lower Cretaceous formations flow out from several springs (Hammam el Malih (HEM), Ein el Jamal, and El Hamma) and from boreholes Mehola 5 and Argaman (Figure 1). All these sources are concentrated in an area which is densely faulted. All springs are thermal and emerge along faults. HEM flows out from volcanic rocks exposed by faulting in the core of the anticline. In the MJ1 borehole, swabbing in Lower Cretaceous beds was carried out in the 1228-1232.5 m depth interval. By comparing the chemical parameters (Table 1), it appears that sources ER51-58 and Mehola 5 (at 265 m) relate to the same hydrochemical family which includes also the water of springs Hammam el Malih and Ein el Jamal and the water in all northern Argaman wells. As confirmed by PHREEQC inverse modeling, the chemistry of water from Lower Cretaceous formations could have been formed by natural mixing of Upper Jurassic brine with freshwater as exploited at present from well Beqaot 2.

The water encountered in the deeper parts of the Kurnub Group (sample ER58) was more saline (7.38 g Cl^-/l) than the water in Upper Jurassic beds (4.07 g Cl^-/l) encountered at a 500 m deeper level (ER51) (Table 4). This "inverse phenomenon" could have been caused by the close vicinity to the major fault which caused the previously mentioned stratigraphic lacuna. This major disturbance could have created a conduit facilitating the interaquifer connection. The high pressures were probably the driving force raising the deep hot brine (72°C) to 1280 m. This geothermal anomaly disappeared at a later stage when the casing was lowered closing the interconnecting fault zone. The chemical parameters indicate that the saline water (7.38 g Cl^-/l) encountered in the Kurnub Group beds was the product of dilution of the Upper Jurassic brine sampled on 7.11.2018 (27.9-50.9 g

Table 4: Comparison of chemical compositions from the Upper Jurassic to Lower Cretaceous beds with groundwater from the adjacent Mehola 5 borehole.

Parameter	Mehola 5 Lower Cretaceous, 265 m	Swab ER58 Lower Cretaceous, 1228-1232 m	Swab ER51 Up. Jurassic zone, 1775-1784 m
Cl^- (mg/l)	2698	7383	4071
SO_4^{2-} (mg/l)	219	652	471
HCO_3^- (mg/l)	220	238	197
SiO_2 (mg/l)		46	58
Na/Cl	0.77	0.8	0.7
*r*Mg/Ca	0.32	0.4	0.4
*r*Q	2.02	2.9	3.0
*w*Cl/Br	112	98	67

r = meq/l; *w* = mg/l.

Cl^-/l). The Cl^- concentrations are similar to those measured in springs and water wells in the area.

The Ha'On brine with $Mg^{2+} > Ca^{2+}$ which is encountered along the eastern and southern shores of Lake Kinneret represents seawater which invaded the Rift and underwent about 37% evaporation (derived from data according to McCaffrey et al. [36]). In spite of different Ca^{2+}/Mg^{2+} values, the similarity of Na^+/Cl^-, Cl^-/Br^-, and $(Ca^{2+}+Mg^{2+})/Na^+$ values suggest that the Ha'On brine or any of its diluted equivalents was converted into the Tiberias brines outflowing along the western rims of the Rift. Under the given petrologic conditions with alkaline olivine basalt flows covering the Tertiary limestones south of Tiberias, it is reasonable to infer that the chemical evolution of Ha'On into Tiberias brines is the result of dolomitization of limestones and alteration of plagioclase to albite, illite, and chlorite. Halite and gypsum are enhanced either by leaching evaporites or by mixing with an evaporite dissolution brine of corresponding composition [34]. A third trend leads to Ha'On and THS brines occurring close to Lake Tiberias. Their compositions indicate a lesser degree of evaporation of Tertiary seawater and dilution by freshwater than in the case of the Triassic brines.

The subsurface geological structure of the Bet She'an Valley area is dominated by an intricate system of major faults and fissures related to the Rift system. Notwithstanding the dense network of faults in the subsurface of the Bet She'an Valley, there are no indications for upflow of deep-seated Triassic-Lower Jurassic brines into the overlying Lower Cretaceous-Lower Miocene sequence. In view of this evidence, it is clear that along the MJ1 borehole and in the surrounding areas, there are several well-defined, separate, and easily identifiable bodies of groundwater in the salinity range of brine to brackish. The thermal gradient in the Lower Cretaceous-Lower Miocene sequence is considerably lower than that in the deeper (Jurassic-Triassic) formations. This is due to the cooling effect caused by contemporary recharge by precipitation on exposed replenishment areas on Mt. Gilboa and on the Fari'a-Beqaot anticline.

6.7. Geochemical Families. In the Rift and in adjoining areas, there are two definite source brines: the Triassic brine and the Late Tertiary one, also known as the Rift brine [3].

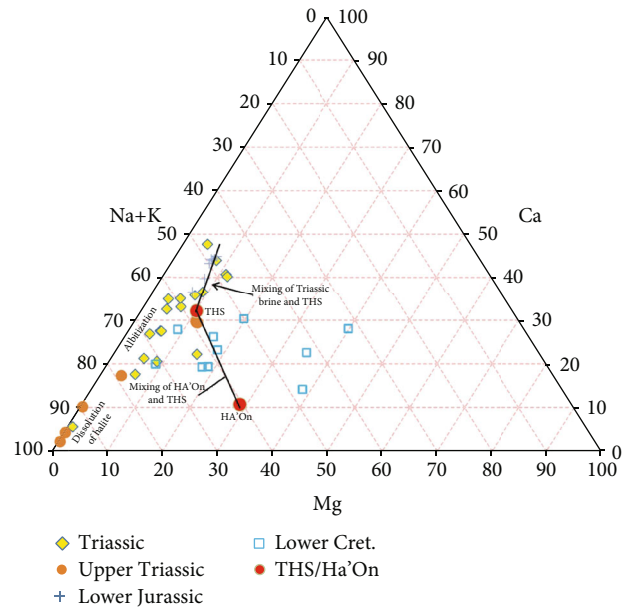

Figure 7: Triplot of brines (data in Table 1) indicating the dissolution of halite and dolomite, alteration of Ha'On brine into THS, and mixing of Triassic brine and THS. Except for the Tertiary Ha'On-THS brines, all the others are grouped according to their beds of occurrence. Percentages are based on meq/l.

The Tertiary Ha'On-Tiberias family is neither a derivative of Jurassic brines nor a derivative of Triassic brines but is a separate entity [34]. The brines encountered in Jurassic and Cretaceous beds represent ancient mixtures of Triassic and Tertiary brines involving various water-rock chemical transformations The arrows on the triplot point to compositional changes due to dissolution of halite, albitization of plagioclase, dolomitization of limestone, dissolution of dolomite, and mixing of Triassic brine and THS (Figure 7).

The deep brine in borehole Devora 2A (4836-4864 m; 123.4 g Cl^-/l) plots together with the 5000 m brines in borehole MJ1 suggesting common Triassic origin (Figure 5). The deep Rosh Pinna brine has similar genetic roots like the Triassic and Lower Jurassic brines encountered in MJ1 suggesting common Triassic origin. Hence, the deep brines

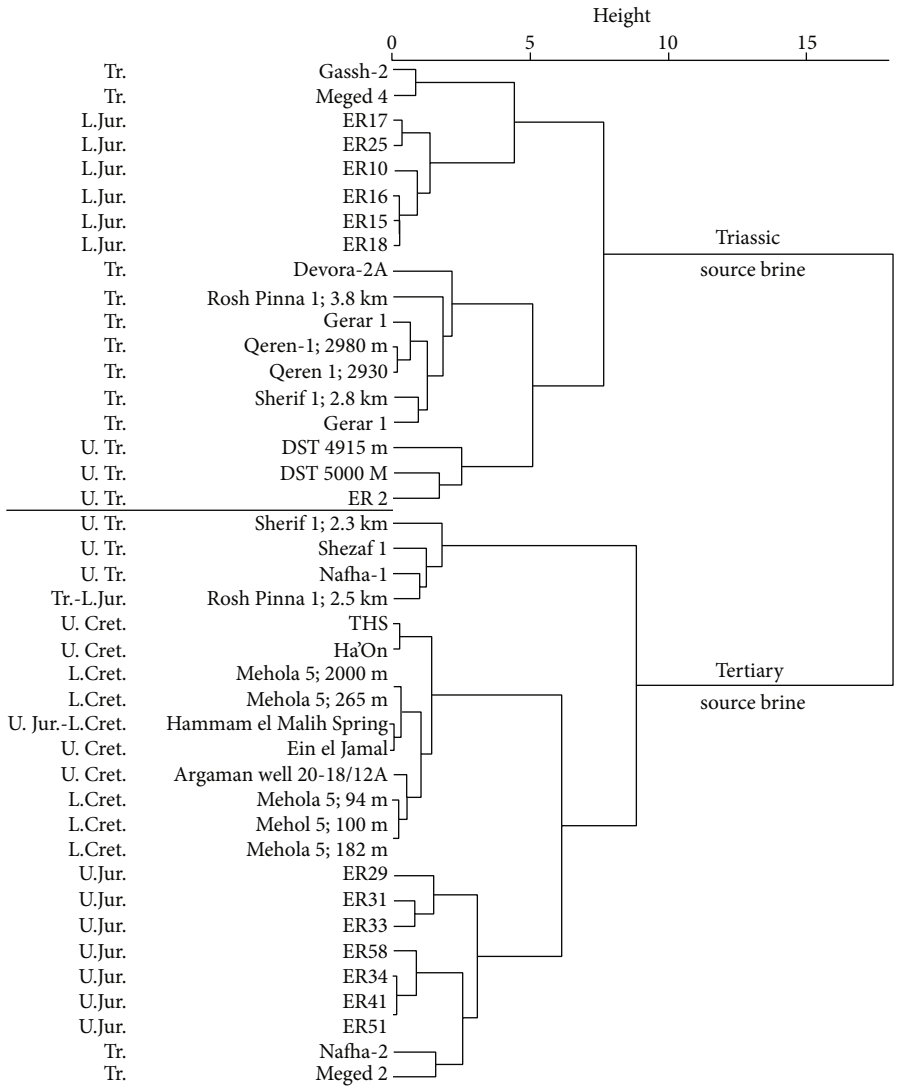

Figure 8: Dendrogram of brines presented in Table 1. The height or distance describes the dissimilarities of the indicated groups. The upper main group of Triassic brines dissimilates to the lower one representing the Tertiary ones.

encountered in boreholes MJ1, Devora 2A, and Rosh Pinna 1 form a tightly connected regional hydrochemical family. This is also backed up by the dendrogram (Figure 8). Though of similar origin, the brines of Devora 2A and Rosh Pinna had further histories of their own. Whereas the Rosh Pinna brine was diluted by THS water, such a process was not observed in the brine of Devora 2A. The Lower Jurassic samples of MJ1 and shallow and low TDE Rosh Pinna brine plot on the same dilution line of the Triassic and the probably freshwater-diluted Ca^{2+}-Cl^{-} THS brine of the Ha'On/Tiberias brine family. The dilution by these brines could have occurred during the Pleistocene, and therefore, the dilution of the shallow Rosh Pinna brine is also a very young process (Figure 4). All diagrams in Figure 5 indicate by red lines a close association and a fixed relationship between the Tiberias Hot Springs (THS) brines and the diluted Rosh Pinna brine.

6.8. Implications on Regional Water Management. The Ca^{2+}-Cl^{-} brine penetrating into the pristine (currently replenished) groundwater in springs and water wells causing their salinization is the Miocene Rift Brine and not the older (Jurassic and Triassic) brines which were discovered and thoroughly documented in borehole MJ1. This most important conclusion is valid not only for the area of the Bet She'an and Harod Valleys but also for the whole Central Jordan Valley including Lake Kinneret with its severe salinization problems. The factor common to all brines in the region is the very high hydraulic pressures. To the present date, there are no clear answers to the question on the factors generating the very high hydraulic pressures (up to several hundred atmospheres) which mobilize the brines originating in deep-seated formations. We may infer heavy lithostatic pressures or structural pressures in the immediate vicinity of the transfer. Very high pressures have been previously reported in wildcat Devora 2A and in other wildcats and were now clearly confirmed for wildcat MJ1. In wildcat Rosh Pinna 1, the pressure release tests were not brought to completion and maximal pressure was not attained. However, in the

partial test, the water rose from the depth of 3864 m to 566 m (-242 m below MSL), i.e., under the pressure of 330 atm (personal communication by N. Schlein to Rosenthal 1988). Hence, the data from these three deep boreholes indicates a mechanism in which the deep brines are piston-driven upwards and possibly also laterally.

Until recently, there were two main obstacles to developing and managing fresh groundwater resources in areas structurally related to the Rift. These obstacles were a lack of information on the possible presence of brines in the subsurface and of their hydraulic heads. The recently acquired information (on subsurface structures, hydrochemical stratigraphy, and pressures) supports water planners with precious information.

Another important aspect is the massive development of water desalination plants intended to replace groundwater, the salinity of which deteriorated during the last decades due to penetration of brines. Wildcat MJ1 revealed the existence of very great volumes of brackish groundwater (<10 g Cl^-/l) which could be used for desalination. Unfortunately, the low permeabilities characterizing Lower Jurassic and Triassic beds do not facilitate disposal of the industrial brine produced during the process of desalination. Moreover, the high artesian pressures which were discovered in the subsurface will push up and out any injected liquid, thus causing major environmental damage. Therefore, the main efforts should be concentrated on the removal of desalination brine, whereas the availability of brackish brine serving as a raw material for desalination does not present any difficulty.

7. Conclusions

The hydrogeological and hydrochemical data collected during the drilling of wildcat MJ1 significantly improved the understanding of groundwater salinization in the Rift and in the structurally connected areas.

For the first time, there is a very clear stratigraphic picture of permeable and nonpermeable strata (aquifers and aquicludes) in the subsurface of the area which are well separated by impervious strata of clays or shales. The various tests proved that the saline groundwater bodies along the MJ1 borehole are characterized by specific and well-defined hydraulic heads and are not fused into a unique and big mass of brine. The difference in the thermal gradient between the Jurassic and Cretaceous formations is a clear indication of isolation and separation between the upper and younger stratigraphic section and the deeper Jurassic-Triassic beds.

In view of this evidence, it is clear that along the MJ1 borehole and in the surrounding areas, there are several well-defined, separate, and easily identifiable bodies of groundwater in the salinity range of brine to brackish. Their distribution along the stratigraphic column is due to their specific gravity, and there is no evidence of interformational mixing. The hydrochemical evidence proves unequivocally that in the subsurface of the drilled area, there are two source brines and two brines which evolved as the result of their mixing and rock-water interaction. Each of these well-separated brines can be easily identified by their chemical composition.

The two source brines are as follows:

(i) The evaporative brine formed during the Triassic and now stored in the Upper Triassic Mohilla formation

(ii) The Late Tertiary (so-called) Rift brine

The two brines which derived from their mixing and chemical transformations and may be identified by their characteristic and different chemistries and hydraulic heads are as follows:

(i) The marine Lower Jurassic brine occurring below the Rosh Pinna shales

(ii) The Upper Jurassic brine is clearly separated from the previous (deeper) one by the Rosh Pinna shales

(iii) The Jurassic saline waters are dilutions of seawater (no evaporation) with the dissolution of small amounts of sulfates. The brines in boreholes Devora 2A and Rosh Pinna may have the same geochemical source as in borehole MJ1, i.e., evaporated Triassic seawater with the dissolution of large amounts of carbonates

The Mehola Group represents diluted seawater. The water emerging from Ha'On and THS are derivatives of evaporated Tertiary seawater and dilution with freshwater. The increase of Ca^{2+} in THS is due to the dolomitization of limestones.

The results of the present study bear on issues of regional water management. It occurs that salinization of regional pristine groundwater in springs and wells is caused only by the Miocene Rift brines which were encountered in the upper horizons of the regional hydrochemical stratigraphy. The older (Jurassic or Triassic) brines are hitherto not involved in such a process. The very high pressures preclude the development of desalination projects because they exclude the disposal of brines by injection into deep-seated strata.

Data Availability

All data used to support the findings of this study are included within the article in the relevant tables. For any data or explanation of data, please write to the senior author.

Conflicts of Interest

I herewith declare that during the research activities and while preparing our manuscript 9812597 for publication, between the authors or between them and any other parties, there were no conflicts of interests in the domains of finances, affiliations, and intellectual properties and of any personal, ideological, academic, or other aspects.

Acknowledgments

The authors are deeply indebted to Zion Oil and Gas, Inc., for their help, consideration, and deep interest in the regional problems of salinization. Many thanks are due to Afikey

Maim-Emeq Ha'Maayanot (Bet She'an Water Supply Co.), its director Mr. Ran Bin-Nun, and Mr. Gadi Gal for supporting, financing, and helping in all activities related to elucidating the hydrochemistry and hydrology of brines encountered during the drilling of wildcat MJ1. They became great friends and spared no effort to facilitate our work. Special thanks are due to the team of the Geochemical Laboratory of the Geological Survey of Israel in Jerusalem and to its head Dr. Naomi Porat for their excellent analytical work, special advice, and friendly attitude. Many thanks and deep appreciation to Dr. Boaz Arnon who interpreted water salinity from the logs.

References

[1] A. Vengosh and E. Rosenthal, "Saline groundwater in Israel; its bearing on the water crisis in the country," *Journal of Hydrology*, vol. 156, no. 1-4, pp. 389–430, 1994.

[2] E. Rosenthal, "Hydrochemical changes induced by overexploitation of groundwater at common outlets of the Bet Shean-Harod multiple-aquifer system, Israel," *Journal of Hydrology*, vol. 97, no. 1-2, pp. 107–128, 1988.

[3] M. Goldschmidt, A. Arad, and D. Neev, "The mechanism of saline springs in the Lake Kinneret depression," *Bulletin - Geological survey of Israel*, vol. 45, pp. 1–19, 1967.

[4] A. Starinski, *Relationship between Ca-chloride brines and sedimentary rocks in Israel, [Ph.D. thesis]*, Hebrew University, Jerusalem, Hebrew, 1974.

[5] M. Gardosh and I. Brunner, "Seismic survey in the Bet She'an region," Report of the Geophysical Institute of Israel 348/27/98, Tel Aviv, Israel, 1998.

[6] P. Möller, C. Siebert, S. Geyer et al., "Relationship of brines in the Kinneret basin, Jordan-Dead Sea Rift Valley," *Geofluids*, vol. 12, 189 pages, 2011.

[7] R. Core Team, "R: a language and environment for statistical computing," R Foundation for Statistical Computing, Vienna, Austria, 2020, https://www.R-project.org/.

[8] Y. Eyal, "Stress-field fluctuations along the Dead Sea Rift since the Middle Miocene," *Tectonics*, vol. 15, no. 1, pp. 157–170, 1996.

[9] M. Meiler, H. Shulman, A. Flexer, M. Reshef, and A. Yelin-Dror, "A seismic interpretation of the Bet She'an basin," *Israel Journal of Earth Sciences*, vol. 57, pp. 11–19, 2008.

[10] B. Arnon, "MJ1-review of possible water aquifers and salinity via log analysis methods," LTRO Consulting Co., Internal Report for Zion Oil Co, Tel Aviv, Israel, 2018.

[11] S. Joffe and Z. Garfunkel, "Plate kinematics of the circum Red Sea - a re-evaluation," *Tectonophysics*, vol. 141, no. 1-3, pp. 5–22, 1987.

[12] Z. Garfunkel, "Lateral movement and deformation along the Dead Sea Transform," in *Dead Sea Transform Fault System: Reviews*, Z. Garfunkel, Z. Ben Avraham, and E. Kagan, Eds., pp. 109–150, Springer Verlag Dordrecht, Heidelberg, New York, London, 2014.

[13] R. Freund, Z. Garfunkel, I. Zak, M. Goldberg, T. Weissbrod, and B. Derin, "The shear along the Dead Sea Rift," *Philosophical Transactions for the Royal Society of London. Series A, Mathematical and Physical Sciences*, vol. 267, pp. 107–130, 1970.

[14] Z. Garfunkel and G. Almagor, "The continental margin of northern Israel," *Geological Survey of Israel Current Research*, pp. 95-96, 1981.

[15] A. Sneh and R. Weinberger, "Major structures of Israel and Environs, scale 1:500,000," *Geological Survey of Israel*, 2014.

[16] N. Joseph-Hai, Y. Eyal, and R. Weinberger, "Mesoscale folds and faults along a flank of a Syrian Arc monocline, discordant to the monocline trend," *Geological Society, London, Special Publications*, vol. 341, no. 1, pp. 211–226, 2010.

[17] R. Weinberger, M. R. Gross, and A. Sneh, "Evolving deformation along a transform plate boundary: example from the Dead Sea fault in northern Israel," *Tectonics*, vol. 28, article TC5005, 2009.

[18] M. Politi, *A comparison of fractures from outcrops and boreholes derived from a 3D seismic column, [Ph.D. thesis]*, Hebrew University of Jerusalem, Jerusalem, Israel, 2019, (in preparation).

[19] B. Derin, *The Subsurface Geology of Israel –Up. Paleozoic to Up. Cretaceous*, Published by author, Rehovot, Israel, 2016.

[20] Y. Zak, *The geology of Mt. Sdom, [Ph.D. thesis]*, Dept. of Geology, Hebrew University, Jerusalem, Israel, 1967.

[21] K. Bandel and H. Khoury, "Lithostratigraphy of the Triassic in Jordan," *Facies*, vol. 4, no. 1, pp. 1–26, 1981.

[22] Z. R. Beydoun and J. G. Habib, "Lebanon revisited: new insights into Triassic hydrocarbon prospects," *Journal of Petroleum Geology*, vol. 18, no. 1, pp. 75–90, 1995.

[23] S. Ben-Zaqen, "Devora 2A completion report," Oil Explor. (Investment) Co., Ltd Rep,78/1, Tel Aviv, Israel, 1978.

[24] Y. Greitzer, "Hydrodynamic investigation of geological formations in Israel to the purpose of oil exploitation – stage 1," *Geological and Hydrological Projects*, vol. 1-2, pp. 1–210, 1980.

[25] Y. K. Bentor, "On the evolution of subsurface brines in Israel," *Chemical Geology*, vol. 4, no. 1-2, pp. 83–110, 1969.

[26] J. Coates, E. Gottesman, N. Jacobs, and E. Rosenberg, "Gas discoveries in the western Dead Sea region," *World Petroleum Congress*, vol. 6, no. 26, pp. 21–36, 1963.

[27] O. Buch-Leviatan, L. Roter-Schindler, and M. Politi, "Miocene normal faulting in the Bet Shean area indicated by the Megiddo-Jezreel 1 well," 2018.

[28] Y. Bartov, "Developments in the geology of the Dead Sea Rift," *TevaVa'Aretz*, vol. 25, pp. 30–35, 1983.

[29] F. Bender, *Geologie von Jordanien*, p. 196, 1974.

[30] L. Damesin, "Geological report Petroleum Development (Palestine) Ltd," 1933.

[31] P. Möller, P. Dulski, S. Geyer, E. Rosenthal, Y. Guttman, and E. Salameh, "Hydrochemistry of groundwater on both sides of the Jordan-Dead Sea-Arava Transform fault," 2005.

[32] A. S. Alshaharan and A. E. M. Nairn, *Sedimentary Basins and Petroleum Geology of the Middle East*, Elsevier, Amsterdam, 1997.

[33] E. Rosenthal and S. Mandel, "Hydrological and hydrogeochemical methods for the delineation of complex groundwater flow systems as evidenced in the Bet-Shean Valley, Israel," *Journal of Hydrology*, vol. 79, no. 3-4, pp. 231–260, 1985.

[34] P. Möller, E. Rosenthal, N. Inbar, and C. Siebert, "Development of the inland sea and its evaporites in the Jordan-Dead Sea transform based on hydrogeochemical considerations and the geological consequences," *International Journal of Earth Sciences*, vol. 107, no. 7, pp. 2409–2431, 2018.

[35] F. J. Alcala and E. Custodio, "Using the Cl^-/Br^- - ratio as a tracer to identify the origin of salinity in aquifers in Spain and Portugal," *Journal of Hydrology*, vol. 359, no. 1-2, pp. 189–207, 2008.

[36] M. A. McCaffrey, B. Lazar, and H. D. Holland, "The evaporation path of seawater and the coprecipitation of Br^- and K^+ with halite," *Journal of Sedimentary Petrology*, vol. 57, pp. 928–937, 1987.